doi: 10.1016/j.joule.2019.02.003

Understanding Continuous Lithium-Mediated Electrochemical Nitrogen Reduction

Nikifar Lazouski,[1] Zachary J Schiffer,[1] Kindle Williams,[1] and Karthish Manthiram[1]*

[1]Department of Chemical Engineering; Massachusetts Institute of Technology; Cambridge, MA 02139, USA

*Corresponding Author: karthish@mit.edu

doi: 10.1016/j.joule.2019.02.003

Summary

Ammonia is a large-scale commodity chemical that is crucial for producing nitrogen-containing fertilizers. Electrochemical methods have been proposed as renewable and distributed alternatives to the incumbent Haber-Bosch process, which utilizes fossils for ammonia production. Herein, we report a mechanistic study of lithium-mediated electrochemical nitrogen reduction to ammonia in a non-aqueous system. The rate laws of the main reactions in the system were determined. At high current densities, nitrogen transport limitations begin to affect the nitrogen reduction process. Based on these observations, we developed a coupled kinetic-transport model of the process, which we used to optimize operating conditions for ammonia production. The highest Faradaic efficiency observed was 18.5 ± 2.9%, while the highest production rate obtained was $(7.9 \pm 1.6) \times 10^{-9}$ mol cm^{-2} s^{-1}. Our understanding of the reaction network and the influence of transport provides foundational knowledge for future improvements in continuous lithium-mediated ammonia synthesis.

doi: 10.1016/j.joule.2019.02.003

Introduction

Ammonia is one of the most widely produced industrial chemicals, with a worldwide production of 170 million tons per annum.[1] At least 80% of ammonia is used in fertilizer production, making ammonia production critical for agriculture.[2] Today, ammonia is produced predominantly via the Haber-Bosch process, which involves reacting nitrogen and hydrogen over heterogeneous catalysts at high temperatures of 450-500°C and pressures up to 200 atm.[3] Hydrogen gas is typically generated on-site from fossil fuels via steam reforming; this leads to significant carbon dioxide emissions of 1.9-9.3 tons CO_2 per ton of NH_3.[4,5] In total, the Haber-Bosch process consumes approximately 1% of the world's energy supply and emits over 450 million tons of CO_2 per year.[4,6] Because of the harsh operating conditions and on-site hydrogen production, the process is economically viable only at large scales.[7] This makes it difficult to produce ammonia in a modular and distributed manner through Haber-Bosch. Distributed ammonia production, if achieved, could reduce inefficiencies and costs associated with fertilizer distribution.[8]

In order to overcome these challenges, methods to produce ammonia electrochemically from nitrogen and water at ambient conditions have been proposed, which could help to reduce the CO_2 footprint of the process. Operating at ambient conditions without the use of steam reforming enables smaller scale processes with lower capital costs.[9] The reduced CO_2 footprint and capital costs, as well as the economics associated with distributed production, can make electrochemical reduction competitive with industrial Haber-Bosch in certain contexts. Many catalyst chemistries have been proposed for electrochemical nitrogen reduction, including structured noble metals,[10] metal oxides,[11] metal nitrides,[12] metal sulfides,[13] nitrogen- and boron-doped carbon,[14] and lithium metal.[15–19] Despite the large variety of reported catalysts, many of

doi: 10.1016/j.joule.2019.02.003

them exhibit low Faradaic efficiencies (FEs) and rates for producing ammonia, often below 10% and 10^{-10} mol cm^{-2} s^{-1}, respectively (Table S1).[19,20]

Among these chemistries, lithium metal-based methods report some of the highest FEs (Table S1).[15–18] Lithium metal is unique in that it can undergo a bulk reaction in which it spontaneously splits the nitrogen triple bond at ambient conditions.[21] In lithium-mediated nitrogen reduction, lithium ions are reduced to lithium metal, which spontaneously reacts with nitrogen to form lithium nitride. The lithium nitride then reacts with a proton source to form ammonia. High FEs in lithium-mediated nitrogen reduction were often achieved by running the process in a batchwise fashion,[16–18] at elevated pressures,[15] or at elevated temperatures at certain steps.[16,18] It would be attractive to produce ammonia continuously at ambient temperatures and pressures. In this vein, a continuous method has been reported in which lithium metal is plated onto metal electrodes from a 0.2 M lithium perchlorate, 1% ethanol in tetrahydrofuran solution in the presence of nitrogen to produce ammonia.[15] However, mechanistic understanding of this process is lacking, which makes it difficult to rationally improve the process yields.

Herein, we report a mechanistic study of continuous lithium-mediated ammonia production at room temperature and pressure. We determined the rate laws of the two main rate-limiting reactions in the system: the reaction between lithium and ethanol to form hydrogen (lithium protolysis) and the reaction between lithium and nitrogen to form lithium nitride (lithium nitridation), from which ammonia is evolved. These rate laws were integrated into a coupled kinetic-transport model that incorporated the competing reactions in a simple reaction network. The model is able to explain experimental results with great fidelity. The model also suggests that transport limitations can be observed in the system for nitrogen reduction, demonstrating the fast intrinsic kinetics of the lithium-mediated approach. Through a series of improvements in

doi: 10.1016/j.joule.2019.02.003

experimental setup, including utilization of a separator, drying of solvents, purification of reagents, and galvanostatic operation, and through mechanistic understanding of the process, we obtained high ammonia FEs and rates at ambient conditions. The maximum FE and production rate obtained were 18.5 ± 2.9% and 7.9 ± 1.6 × 10^{-9} mol cm^{-2} s^{-1}, respectively.

doi: 10.1016/j.joule.2019.02.003

Results

Electrochemical Approach

The lithium-mediated nitrogen reduction cycle was run continuously in a 2-compartment electrochemical cell (Figure 1, S1, S2). In this setup, lithium metal is plated onto an inert metal substrate from solution in a polar, aprotic solvent. Nitrogen gas dissolved in the electrolyte reacts with the plated lithium to form lithium nitride. The nitride reacts with the proton carrier, here ethanol, to form ammonia that remains dissolved in the electrolyte.

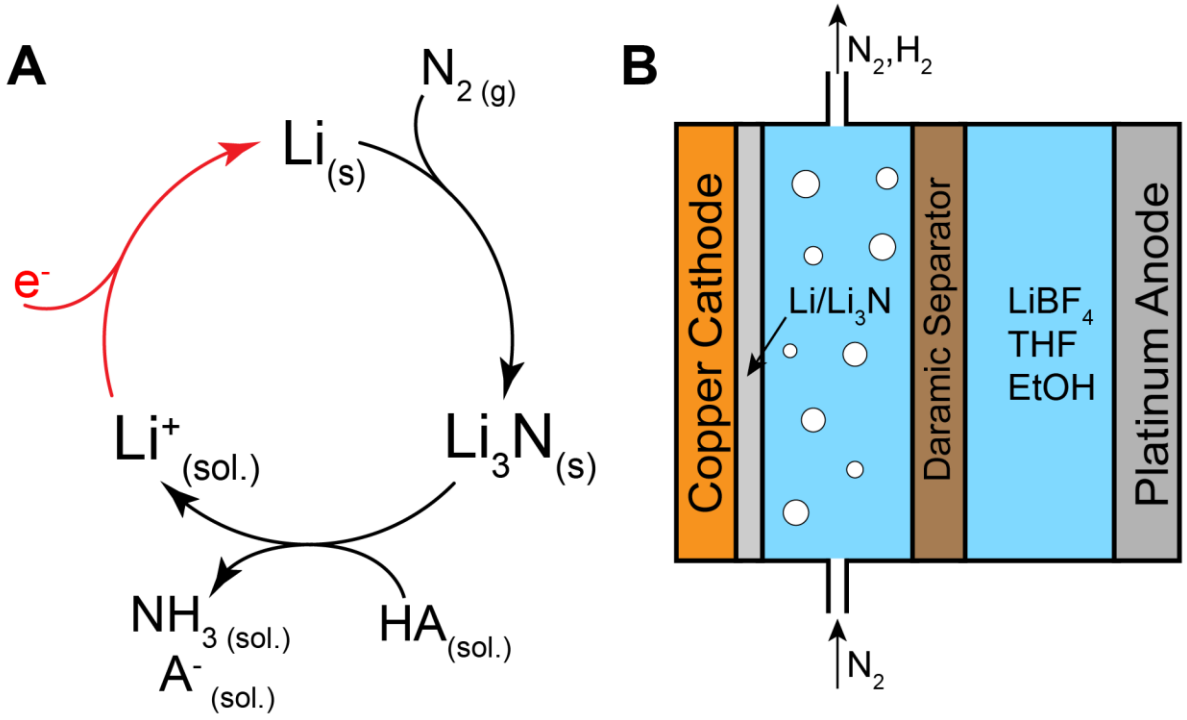

Figure 1. Lithium-mediated nitrogen reduction to ammonia. (A) The chemistry involved in ammonia synthesis. Compound subscripts denote phases; (s) is solid, (g) is gas, (sol.) is solution phase. (B) The electrochemical cell setup used in the described experiments.

doi: 10.1016/j.joule.2019.02.003

Control Experiments

It is imperative to verify that detected ammonia is a result of N_2 reduction and does not originate from either adventitious sources or contaminants.[4,22] We performed a series of control experiments in order to confirm N_2 reduction (Figure 2). The concentration of ammonia in the cell was found to increase with time when applying a constant current, as determined by taking periodic aliquots from a single operating cell (Figure 2A), which supports the assertion that ammonia is generated during electrolysis and is not present as a contaminant before the experiment. As HNO_3 is used in preparing the cathode (see SI Experimental Procedures), we sought to rule out nitrate reduction as the source of ammonia. When HCl-etched and unetched copper foils were used as the cathode, ammonia is still detected, confirming that contamination from HNO_3 etching is not responsible for ammonia formation (Figure S6). When argon was used as the feed gas, little ammonia was detected (Figure 2B); the ammonia that was detected in this argon control was likely produced due to residual nitrogen in the cell (see SI Experimental Procedures). This confirms that the presence of dinitrogen is required for ammonia generation.

Isotopic labeling of nitrogen allowed us to directly trace conversion of dinitrogen to ammonia.[4,23–26] When isotopically labelled nitrogen gas, $^{15}N_2$, was used as the feed gas, ammonia was first detected via the colorimetric assay (Figure 2B, S3, S4, S5), then analyzed by NMR. When $^{14}N_2$ was used as the feed gas, a triplet with equal peak intensities was observed at 7.23 ppm with J = 52.2 Hz, corresponding to ^{14}N-^{1}H coupling in NH_4^+ (Figure 2C).[27] The NMR spectrum of the electrolyte solution obtained following electrolysis of $^{15}N_2$ contains a doublet at 7.23 ppm with J = 73.2 Hz, corresponding to ^{15}N-^{1}H coupling in NH_4^+ (Figure 2C),[27] which confirms that ammonia was made from the feed $^{15}N_2$. As ammonia contamination of isotopically labeled nitrogen feedstocks is possible,[28,29] we performed additional control experiments in which both $^{15}N_2$ and

doi: 10.1016/j.joule.2019.02.003

$^{14}N_2$ were fed to the cell in the absence of polarization. No ammonia was detected in either case by NMR or colorimetric assay, confirming the purity of the gas feeds, and further validating that ammonia was formed via nitrogen reduction.

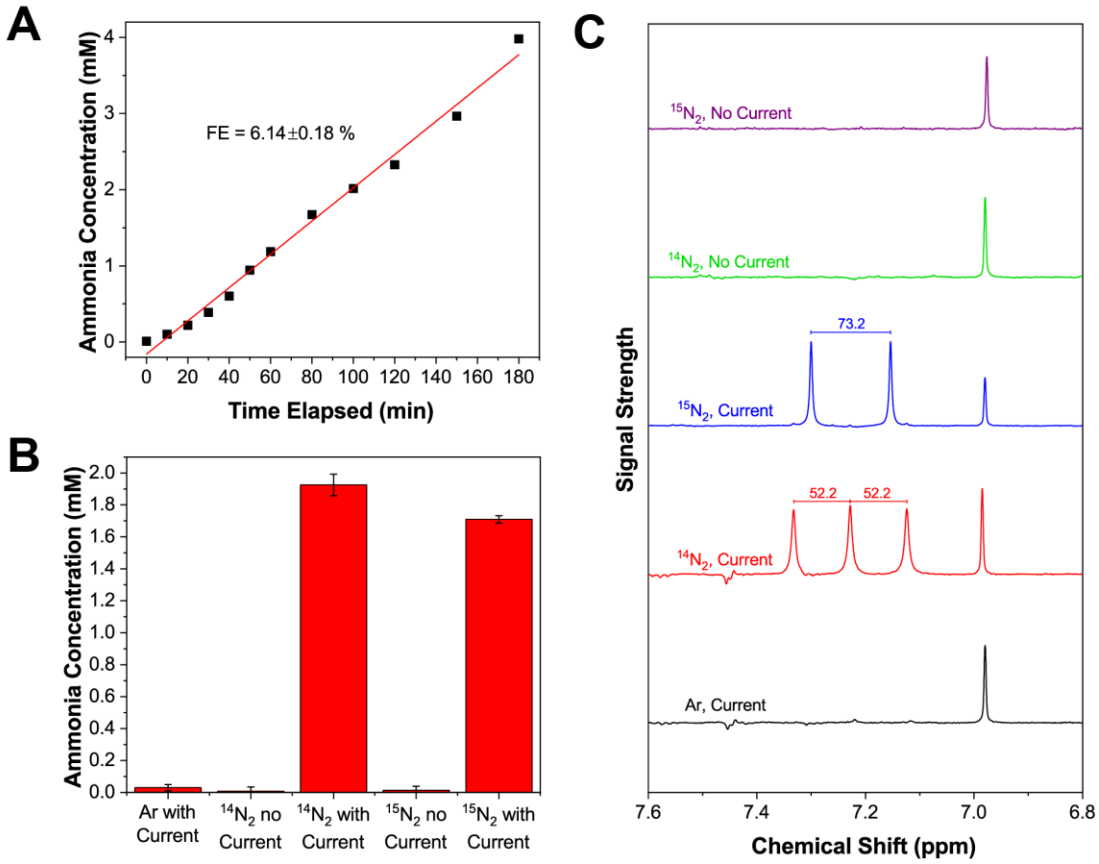

Figure 2. Control experiments confirming ammonia generation via nitrogen reduction. (A) Evolution of ammonia concentration over time in a cell containing 0.2 M EtOH and an applied current density of 3 mA cm^{-2}. (B) Concentrations of ammonia in the electrolyte solutions following experiments in which $^{15}N_2$, $^{14}N_2$, and Ar were used as feed gases as measured by the colorimetric assay. A 15 mA cm^{-2} current was applied for 15 minutes in experiments with current; no current was applied for the same amount of time in the other experiments. Error bars depict the standard deviation in the quantification assay based on n=2. (C) NMR spectra of the solutions from aforementioned experiments. The $^{15}N_2$ plot has been scaled down relative to the other spectra for readability. The different proton splitting patterns spectra resulting from $^{14}N_2$ and $^{15}N_2$ gas feeds support the claim that ammonia comes from the feed gas.

doi: 10.1016/j.joule.2019.02.003

Effect of Nitrogen Concentration on Nitrogen Reduction

As nitrogen is the species that is being reduced, we sought to understand the impact of nitrogen partial pressure on the observed FE towards ammonia. The partial pressure of nitrogen was varied between 0 and 1 bar by diluting the nitrogen stream with argon; the concentration of ethanol in the system was kept constant at 0.2 M and a constant current of 3 mA cm^{-2} was applied to produce ammonia. The FE towards ammonia increased linearly with nitrogen pressure (Figure 3). As nitrogen concentration in solution is proportional to the partial pressure of nitrogen due to Henry's law, we can conclude that the reaction between lithium and nitrogen is first order in nitrogen. The partial current density towards ammonia in these experiments is significantly lower than the transport-limited current density (see Supplemental Information), which implies that the first-order behavior is a manifestation of the kinetics of the process, not the transport. The fact that ammonia yields decrease at lower partial pressures of nitrogen helps to further validate that ammonia comes from nitrogen reduction and not from adventitious sources.

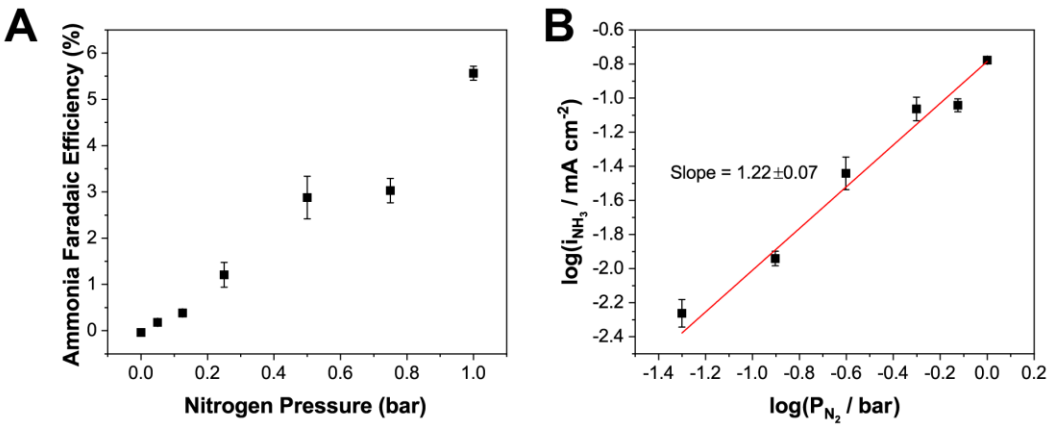

Figure 3. Effect of nitrogen partial pressure on ammonia production. Variation in (A) Faradaic efficiency and (B) production rate towards ammonia with varying partial pressures of N_2. The partial pressure was controlled by diluting N_2 with Ar. When no N_2 was present, no ammonia was detected. Error bars represent the standard deviation between replicates of the same experiment with n = 3.

doi: 10.1016/j.joule.2019.02.003

Effect of Proton Carrier Concentration

We elucidated the effect of the proton carrier, ethanol, by varying its concentration while holding the nitrogen pressure and current density constant at 1 bar and 3 mA cm^{-2}, respectively. No ammonia or hydrogen was generated in the absence of ethanol, and a significant layer of lithium accumulated on the surface of the cathode (Figure S7); this implies that the applied current goes towards plating lithium which remains unreactive in the absence of ethanol. The ammonia FE initially increases with increasing ethanol concentration and reaches a peak value at 0.1 M, with an average Faradaic efficiency towards ammonia of 7.8 ± 3.0% (Figure 4A, Table S4). At ethanol concentrations >0.1 M, the Faradaic efficiency for ammonia decreases monotonically with ethanol concentration; the main side product under these conditions is hydrogen gas (Figure S15). The rate of ammonia generation exhibits an approximately -1.5 order with respect to ethanol concentration in this regime (Figure 4B). We believe this effect can be explained by a decrease in the amount of lithium available for nitridation at higher ethanol concentrations due to increased competition from direct lithium protolysis by ethanol; this is reflected in the lower coverage of lithium at higher ethanol concentrations (Figure S7A-C).

doi: 10.1016/j.joule.2019.02.003

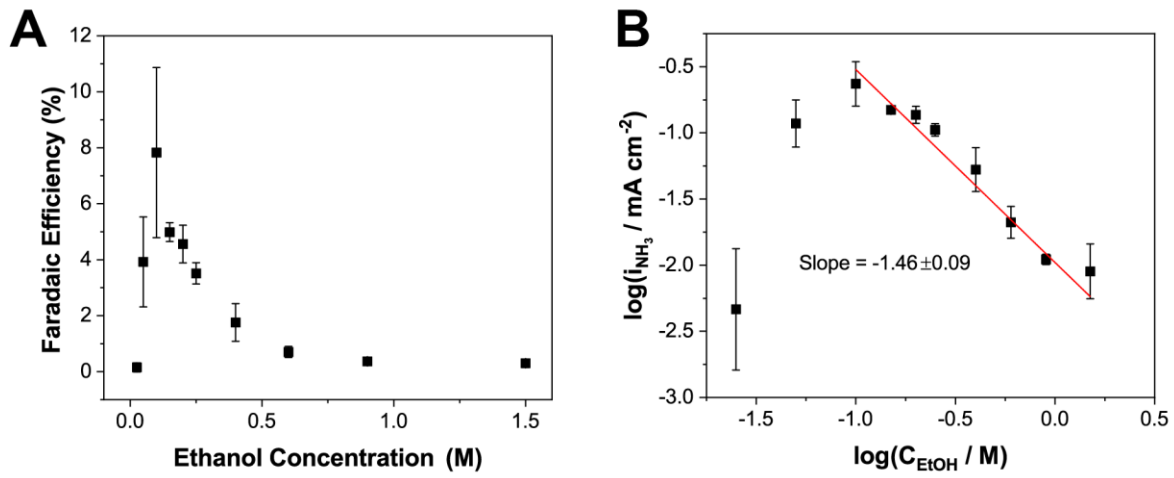

Figure 4. Effect of ethanol concentration on ammonia production. The effect of varying ethanol concentration on (A) the Faradaic efficiency and (B) production rate of ammonia. There is an optimal ethanol concentration at which ammonia yields are maximized. At higher concentrations, ethanol competes with nitrogen to react with lithium, which leads to a negative order with respect to ethanol, as seen in (B). Error bars represent the standard deviation between replicates of the same experiment with n = 3.

It is important to address the economic and practical aspects of using ethanol as a proton carrier for ammonia synthesis. We define the proton carrier to be the species that protonates lithium and lithium nitride in the reactions at the cathode, while the hydrogen source is the species that loses hydrogen atoms in the overall reaction at both electrodes. In this study, ethanol is used as a model proton carrier that can lead to high ammonia yields while forming lithium ethoxide; it is also the hydrogen source. While ethanol is a renewable hydrogen source, as it is produced from biomass, it is not economically viable to use ethanol as the hydrogen source for ammonia synthesis at industrial scales. It would be desirable to use water instead of ethanol as the hydrogen source due to its lower cost. Adding water to the catholyte was found to negatively affect ammonia yields, which may hinder its use as a direct proton source and carrier (Figure S9). In future work, one way to utilize water as the hydrogen source could be by oxidizing it at the anode to produce oxygen gas and protons; the protons could react with free proton carrier and be transported to the cathode

doi: 10.1016/j.joule.2019.02.003

(Figure S17). Alternatively, hydrogen gas sourced from water-splitting could be oxidized at the anode. In both of these setups, ethanol, or any other chosen carrier molecule, would only act as the proton carrier to the cathode and would not be consumed.

Effect of Current Density

In order to study the effect of the rate of lithium plating on the production of ammonia, the applied current density was varied between 0.3 mA cm^{-2} and 25 mA cm^{-2}. The concentration of ethanol in these experiments was held constant at 0.2 M, a concentration higher than the optimal one. This value was chosen in order to maintain a low surface concentration of the plated lithium, which is useful for mechanistic analysis (see Discussion), as well as to obtain results with less variation in FE between runs, since the standard deviation in FE is smaller at ethanol concentrations higher than the optimal one. The FE and rate of ammonia production change significantly with applied current density. The rate for ammonia production increases monotonically with increasing current density (Figure 5C). This implies that the nitride formation rate increases with current density; this is consistent with previously reported observations of faster nitrogen fixation in Li-ion batteries at increased plating current densities.[30] The FE towards ammonia, however, increases with current density only at low current densities Figure 5A). In this region, the FE increases proportionately to the square root of current density. At approximately 15 mA cm^{-2}, the FE reaches a maximum value, with an average FE of 8.6 ± 2.2%. At higher current densities, the FE towards ammonia begins to decrease. We believe that the peak in FE is caused by nitrogen transport limitations, as discussed below.

doi: 10.1016/j.joule.2019.02.003

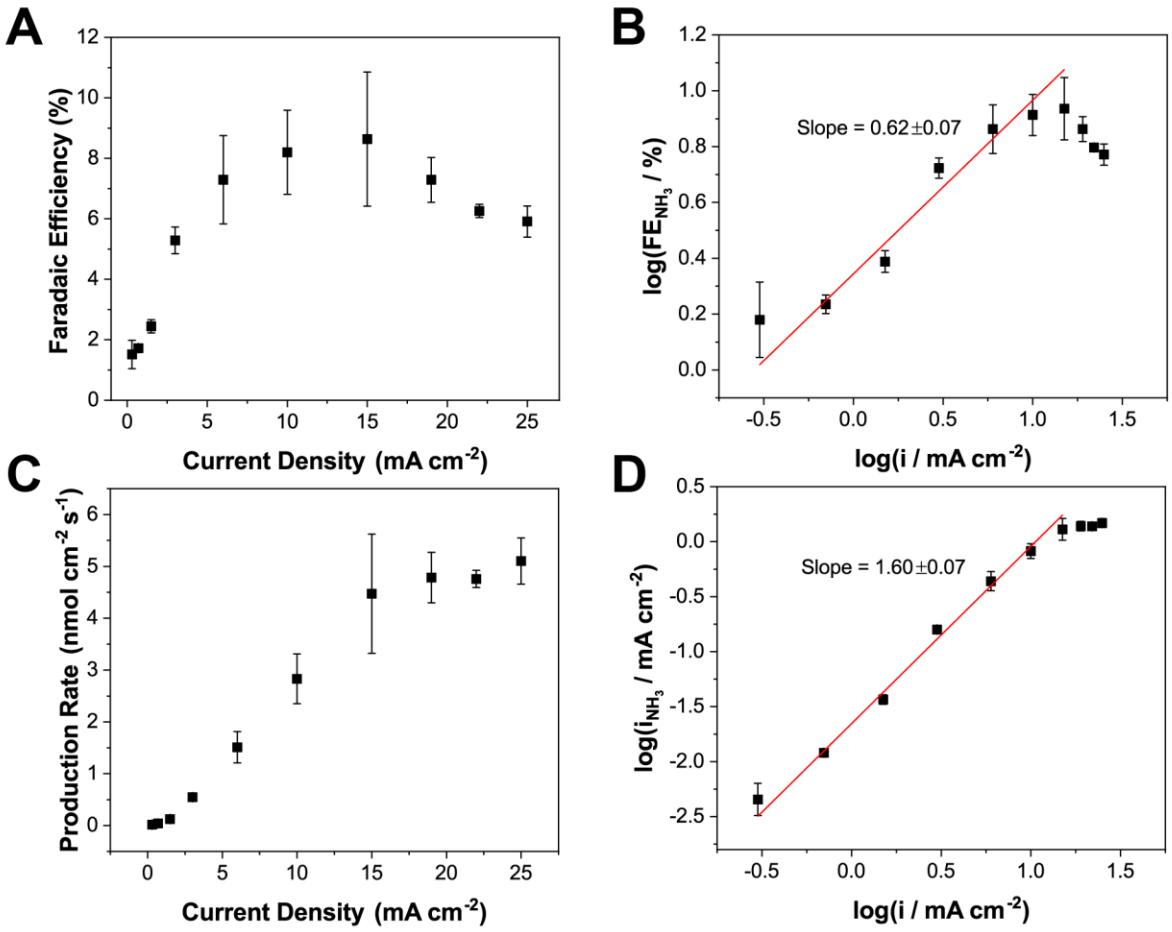

Figure 5. Effect of applied current density on ammonia production. The effect on (A, B) Faradaic efficiency and (C, D) production rate. Initially, the FE increases proportionally to the square root of the current density. At approximately 15 mA cm^{-2}, the FE peaks and begins to decrease. The production rate monotonically increases with current density, but begins to stabilize above 15 mA cm^{-2}. Error bars represent the standard deviation between replicates of the same experiment with n = 3.

Discussion

The existence of an optimal ethanol concentration at which ammonia production is maximized reveals many mechanistic details of ammonia synthesis (Figure 4). The negative order with respect to ethanol at higher ethanol concentrations can be explained by competition between nitrogen and ethanol for reacting with lithium metal and will be discussed in more detail below through our mechanistic model. The reasons for the positive order in ethanol at low concentrations

doi: 10.1016/j.joule.2019.02.003

are less obvious, however. One potential explanation could be that at low concentrations of ethanol, there is insufficient ethanol to protonate lithium nitride that forms when nitrogen reacts with lithium, which leads to accumulation of lithium nitride. Accumulation of material on the cathode surface (Figure S7A) and low hydrogen FEs (Figure S15) at low ethanol concentrations support this hypothesis. However, after dissolving the residual solids in 0.1 M HCl following electrolysis, insignificant amounts of ammonia were detected in the resulting solution (Figure S12). If lithium nitride were present, rapid protolysis by HCl would produce large amounts of ammonia. This suggests that the solids do not contain lithium nitride; instead, they most likely contain unreacted lithium.

Alternatively, at low ethanol concentrations, increasing the ethanol concentration may assist nitride formation. This could occur if higher ethanol concentrations disrupt the solid-electrolyte interphase (SEI) on the lithium.[31] This would expose more fresh lithium for reactions. Another mechanism by which ethanol could assist nitride formation is by causing defects in the structure of lithium. A similar effect has been observed in solid state lithium nitridation, wherein the reaction is accelerated in the presence of small amounts of water vapor.[32] In this case, water vapor acts as a proton source and creates defects at which nitrogen can react.[32] Regardless of the mechanism, increases in ethanol concentration promote reactions between lithium and both ethanol and nitrogen, leading to significantly higher ammonia and hydrogen FEs (Figure 4, S15) than observed in the absence of ethanol.

At high ethanol concentrations, a great deal of mechanistic insight can be extracted from the order of the ammonia production rate with respect to nitrogen and ethanol, as well as from the dependence of FE on current density. In particular, the observed orders with respect to current density and ethanol are non-integer, which implies interactions between elementary reactions. In

doi: 10.1016/j.joule.2019.02.003

order to explain the observed phenomena, we developed a model that describes the reactions of plated lithium with nitrogen or ethanol to form ammonia or hydrogen, respectively. We assume that there is a small amount of lithium on the surface that is constant in time, but can change with operating conditions. This amount is assumed to be significantly lower than the equilibrium amount of lithium defined by the applied potential; the amount is instead defined by the competing lithium formation and consumption reactions after an initial plating time, and can be found by invoking a quasisteady-state approximation (QSSA) for lithium.[33] The amount of lithium per geometric surface area, which is similar to a surface concentration, is denoted by $[Li]$. The assumption of low surface concentration is justified by the associated assumption of high ethanol concentration (Figure S7). The reactions with lithium have rates proportional to the lithium concentration to some power:

$$r_{H_2} = k_1[Li]^{\alpha}[EtOH]^{x} \quad (1)$$

$$r_{NH_3} = k_2[Li]^{\beta}[N_2] \quad (2)$$

Here, the rate constants k_1, k_2 are defined to result in rates in units of current density, i.e. they contain Faraday's constant F and any proportionality constants derived from stoichiometry. The rate constants are assumed to be independent of applied current or potential as they describe thermochemical reactions. $[N_2]$ and $[EtOH]$ are the concentrations of nitrogen and ethanol at the electrode surface, respectively. We assume the nitridation reaction is first order in nitrogen from the measured nitrogen partial pressure data (Figure 3). While this reaction formally generates lithium nitride (Li_3N), we assume that the lithium nitride protolysis reaction is fast, such that the reaction between lithium and nitrogen is rate-limiting. This assumption is supported by a lack of lithium nitride observed in the solids on the cathode after electrolysis (Figures S7, S12). In

doi: 10.1016/j.joule.2019.02.003

addition, to simplify the analysis, we assume that the rate of the ammonia forming reaction is significantly lower than the rate of the hydrogen forming reaction:

$$k_2[Li]^{\beta}[N_2] \ll k_1[Li]^{\alpha}[EtOH]^{x} \quad (3)$$

This assumption is valid as the partial current towards ammonia is approximately an order of magnitude lower than the partial current towards hydrogen at ethanol concentrations above the optimal one (Figure 4, S15).

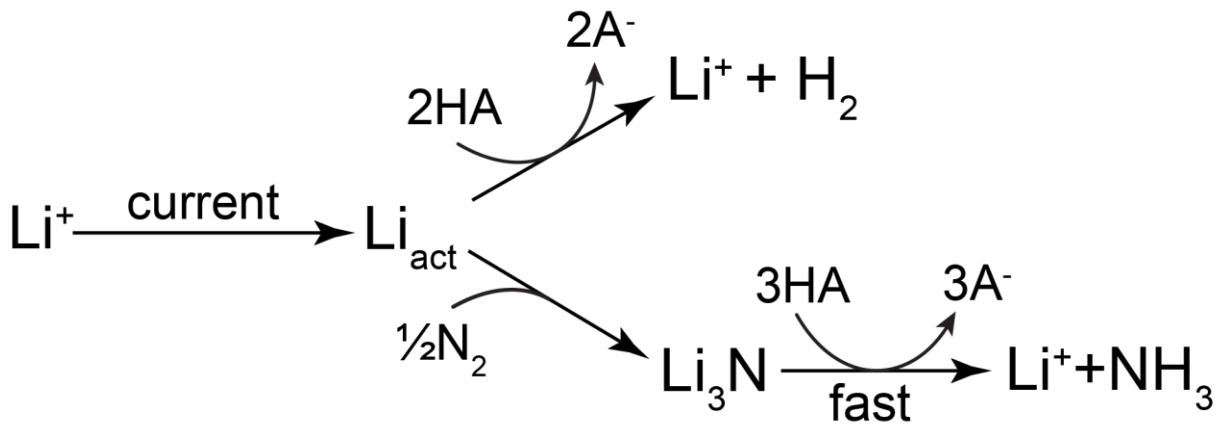

Scheme 1. A visual representation of the reactions assumed to occur in the model. Lithium metal is plated from lithium ions in solution by the application of a current, yielding solid lithium. The lithium metal can react with the proton carrier (HA) to form hydrogen, or with nitrogen to form lithium nitride. Lithium nitride is protonated quickly to form ammonia and does not contribute to measured kinetics; this reaction is kinetically facile and is not probed by our kinetic analyses.

As the experiments were performed galvanostatically, we introduce an applied current density *I* into the model. We have experimentally observed that almost all the current applied goes towards lithium plating; only a small fraction of the current, typically ~1%, goes towards other reactions (Figure S13, S14), likely EtOH or water reduction. For simplicity, we assume all the current goes towards lithium plating in the model. The lithium can then react only via one of the

doi: 10.1016/j.joule.2019.02.003

two aforementioned reactions (Scheme 1); we assume no other side reactions, such as SEI formation, occur. The rate of change of lithium concentration is given by:

$$F\frac{d[Li]}{dt} = I - k_1[Li]^{\alpha}[EtOH]^{x} - k_2[Li]^{\beta}[N_2] \quad (4)$$

From the QSSA assumption made for lithium and the relative rates of ammonia and hydrogen evolution (Eq. 3), the lithium concentration can be solved for in terms of applied current density:

$$I - k_1[Li]^{\alpha}[EtOH]^{x} - k_2[Li]^{\beta}[N_2] \approx I - k_1[Li]^{\alpha}[EtOH]^{x} \approx 0 \quad (5)$$

$$[Li] = \left(\frac{1}{k_1[EtOH]^{x}}\right)^{\frac{1}{\alpha}} I^{\frac{1}{\alpha}} \quad (6)$$

The FE for ammonia can be found to be:

$$FE_{NH_3} = \frac{k_2[Li]^{\beta}[N_2]}{I} \approx \frac{k_2[Li]^{\beta}[N_2]}{k_1[Li]^{\alpha}[EtOH]^{x}} = \left(\frac{k_2}{k_1^{1+\frac{\beta-\alpha}{\alpha}}}\right)\frac{[N_2]}{[EtOH]^{x\left(1+\frac{\beta-\alpha}{\alpha}\right)}} I^{\frac{\beta-\alpha}{\alpha}} \quad (7)$$

According to this model, named the kinetic-only model, the ammonia FE should change with current density as $I^{\frac{\beta-\alpha}{\alpha}}$. Experimental data (Figure 5) suggest that $\frac{\beta-\alpha}{\alpha} = \frac{1}{2}$. One possible interpretation of this result is that $\alpha = 2$ and $\beta = 3$, which corresponds to the number of lithium atoms required to produce one molecule of H_2 or NH_3, respectively.

The model predicts that the ammonia FE should decrease with increasing ethanol concentration, with an order equal to $-x\left(1+\frac{\beta-\alpha}{\alpha}\right) = -x\left(1+\frac{1}{2}\right)$. As the observed order for ethanol from experimental data is -1.5, we can deduce that $x = 1$, from which we infer that the reaction between lithium and ethanol is first order in ethanol. The observed non-integer order for

doi: 10.1016/j.joule.2019.02.003

ammonia FE as a function of ethanol concentration is thus explained by a combination of increased competition from ethanol and decreased availability of lithium to form ammonia.

The FE towards ammonia exhibits a peak as applied current density is varied, which is unexplained by the kinetic model. One explanation for the FE peaking behavior could be a change in the morphology in the plated lithium at higher current densities, and thus a change in its reactivity. Lithium morphology has been observed to change at higher current densities, often turning more dendritic.[34] However, if changes in morphology led to changes in reactivity, the production rate of ammonia could be expected to decrease alongside the FE, which is not observed (Figure 5C).

Alternatively, the lithium concentration could be reaching a maximum possible value at high current densities; this may be reflected in the analytical model as a constant, maximum value of $[Li]$. One of the assumptions made in the model is that the rates of reactions are proportional to the amount of lithium on the surface. This assumption breaks down when lithium is plated rapidly enough to begin plating on top of itself. This could result in a fraction of lithium that cannot contribute to ammonia or hydrogen formation. Visually, there is not a clear difference in the amount of lithium plated at different current densities after electrolysis (Figure S7). However, this does not necessarily disprove this hypothesis, as the difference between thinner and thicker lithium layers may be difficult to observe by visual inspection. In order to reject this hypothesis, we performed an experiment where the concentration of ethanol was decreased to 0.1 M while maintaining the applied current density of 15 mA cm^{-2}, thus increasing the amount of lithium present (Eq. 6). If the lithium concentration was reaching a finite maximum value, then the FE for ammonia would be unaffected. This was not observed; the FE increased to 15.2 ± 3.1% (Figure

doi: 10.1016/j.joule.2019.02.003

6), which is higher than the previously observed value of 8.6 ± 2.2%. Thus, a maximum lithium concentration is not the cause of a peak in ammonia FE.

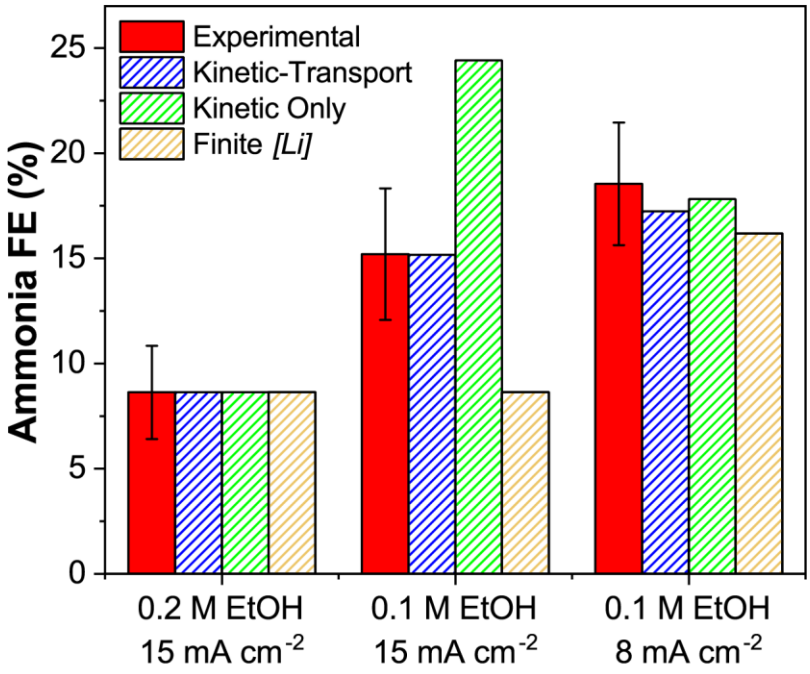

Figure 6. A comparison between proposed kinetic models. The models seek to explain the appearance of an optimum current density to maximize FE. The expressions for the finite lithium concentration model described in the text are given in the Supporting Information. All models use the 0.2 M EtOH, 15 mA cm^{-2} point to fit parameters. Only the coupled kinetic-transport model matches experimental results well under all conditions. Error bars represent the standard deviation between replicates of the same experiment with n = 3.

Another way to explain the observed optimal current density is that the peak is caused by a local decrease of dissolved nitrogen concentration at the electrode surface due to the limited rate of diffusion of nitrogen. In this case, the partial current density for ammonia would be approaching the mass transfer limited current density.[35] While the limiting current (see SI) is significantly higher than the peak partial current towards ammonia (11 ± 8 mA cm^{-2} versus 1.3 ± 0.3 mA cm^{-2}), transport limitations can still be used to explain the peak behavior, as shown by modifying the model below. The rate of diffusion of nitrogen in units of current density to the electrode surface is given by:[35]

doi: 10.1016/j.joule.2019.02.003

$$N_{N_2} = \frac{6FD}{\delta}(C_{bulk} - [N_2]) \tag{8}$$

Nitrogen diffusing to the surface will react with lithium according to Eq. 2. Over time, the system will reach a steady state, in which the concentration profile of nitrogen in the transport boundary layer does not change with time. At this point, the reaction rate of the nitrogen will be equal to its diffusion rate:

$$\frac{6FD}{\delta}(C_{bulk} - [N_2]) = k_2[Li]^{\beta}[N_2] \tag{9}$$

Solving for the concentration of nitrogen at the surface, we obtain:

$$[N_2] = \frac{C_{bulk}}{1 + \frac{\delta}{6FD}k_2[Li]^{\beta}} \tag{10}$$

At this point, we can derive an expression for the FE towards ammonia. We once again assume the partial current for hydrogen is significantly higher than the partial current for ammonia (Eq. 3). The same conclusions are obtained regardless of whether this assumption is made; we make it in order to simplify the resulting expressions. The Faradaic efficiency towards ammonia is given by:

$$FE_{NH_3} = \frac{k_2[Li]^{\beta}[N_2]}{k_2[Li]^{\beta}[N_2] + k_1[Li]^{\alpha}[EtOH]^{x}} \approx \frac{[Li]^{\beta-\alpha}[N_2]}{\left(\frac{k_1}{k_2}[EtOH]^{x}\right)} = \frac{C_{bulk}[Li]^{\beta-\alpha}}{\left(\frac{k_1}{k_2}[EtOH]^{x}\right)\left(1+\frac{\delta}{6FD}k_2[Li]^{\beta}\right)} \tag{11}$$

Substituting the expression for lithium concentration (Eq. 6), we obtain:

$$FE_{NH_3} = \frac{C_{bulk}I^{\frac{\beta-\alpha}{\alpha}}}{\left(\frac{k_1^{\frac{\beta}{\alpha}}}{k_2}[EtOH]^{x\left(1+\frac{\beta-\alpha}{\alpha}\right)}\right)\left(1+\frac{\delta k_2}{6FDk_1^{\frac{\beta}{\alpha}}}\frac{I^{\frac{\beta}{\alpha}}}{[EtOH]^{\frac{\beta}{\alpha}x}}\right)} \tag{12}$$

doi: 10.1016/j.joule.2019.02.003

This model is named the kinetic-transport model. It can be shown that when ammonia FE is maximized by varying the applied current density, the partial current density towards ammonia is one third of the transport limited current density (see Figure S8, Supplemental Information):

$$I_{peak} = \frac{I_{lim}}{3} \quad (13)$$

From this result, we can conclude that the FE towards ammonia can exhibit a peak with respect to applied current density at any fixed ethanol concentration due to transport limitations with a partial current that is only a third of the predicted transport limited current. The partial current towards ammonia at peak FE is 1.3 ± 0.3 mA cm^{-2} (Figure 5), which implies that the limiting current density in the system is 3.9 ± 0.9 mA cm^{-2}. This value lies within the estimated range of possible limiting current densities (11 ± 8 mA cm^{-2}, see SI); hence, it is possible that some transport effects are observed at higher current densities.

The above model predicts that decreasing the ethanol concentration from 0.2 M to 0.1 M while applying 15 mA cm^{-2} increases both the production rate and FE towards ammonia, which was experimentally observed (Figure 6). According to the model, if transport limitations are present, the obtained value of FE is not optimal, as the partial current density towards ammonia is above one third of the transport limited current, which was measured at 0.2 M ethanol (2.3 ± 0.5 mA cm^{-2} vs 1.3 ± 0.3 mA cm^{-2}). Therefore, decreasing the applied current density should increase the Faradaic efficiency. This is, in fact, observed; at 8 mA cm^{-2} and 0.1 M, the Faradaic efficiency increases to 18.5 ± 2.9% (Figure 6), which further supports the hypothesis that nitrogen transport limitations are observed in this system. As lowering the concentration of ethanol further would decrease ammonia production (Figure 4), this FE is close to optimal in this system. Under these conditions, ammonia is produced at an energy efficiency of 1.45%, with most of the energy lost to

doi: 10.1016/j.joule.2019.02.003

resistive dissipation (Figure S16). While we did not explicitly optimize for energy efficiency, it is an important metric to consider when designing electrochemical nitrogen reduction systems.

Conclusion

In summary, this work demonstrates that lithium metal chemistry can be used to fix nitrogen to ammonia continuously in a non-aqueous solvent at high rates at room temperature and ambient pressure. We found that the reaction between nitrogen and lithium is promoted by a small amount of proton carrier, in this case ethanol. We measured rate laws for the reactions between lithium, ethanol, and nitrogen by varying the applied current density and concentrations of relevant species. We found that the lithium nitridation and lithium protonation reactions are first order in nitrogen and ethanol, respectively. The orders with respect to lithium differ for the two reactions, with the nitridation reaction being more sensitive to the amount of lithium present. Due to this difference, the FE towards ammonia was found to increase with increasing applied current density. This finding could potentially allow for development of a process that can produce ammonia at higher FEs. In the present system, the FE for ammonia reaches a maximum value when varying current density while maintaining a high production rate, likely due to nitrogen transport limitations. We hope that mechanistic understanding of this system will serve as a starting point and inspiration for the development of more efficient continuous lithium-mediated methods to produce ammonia.

Experimental Procedures

A polished copper foil served as the cathode, onto which lithium was plated electrochemically; a platinum foil served as the anode; and a polyporous polyethylene separator (Daramic 175) was used to separate the chambers of a PEEK electrochemical cell (Figure S1, S2.

doi: 10.1016/j.joule.2019.02.003

The use of a separator prevented bulk convection of ammonia from the cathode to the anode, at which ammonia may be oxidized (Figure S11). The electrolyte solution consisted of 1 M lithium tetrafluoroborate ($LiBF_4$) dissolved in molecular sieve-dried tetrahydrofuran (THF) with varying concentrations of ethanol (EtOH). A detailed description of the cell geometry, electrolyte preparation procedure, and other experimental details can be found in the Supporting Information. The choice of solvent and proton carrier was based on previous work,[15] while the electrolyte and lithium source were chosen for safety and economic reasons. Many factors are essential to obtain high ammonia yields, including dryness of the solvent (Figure S9), purity of the reagents (Figure S10), and the use of a thick separator (Figure S11).

The cathode compartment of the cell was continuously purged with 10 sccm of THF-saturated N_2 gas both before polarization and during the experiment. Lithium metal was galvanostatically plated onto the copper cathode. The lithium metal reacted continuously with nitrogen dissolved in the electrolyte solution to form lithium nitride, which was subsequently protonated by the ethanol in solution to form ammonia (Figure 1A). The electrolyte solution containing ammonia was diluted with water; the ammonia content of the resulting solution was quantified using the salicylate method.[16,36,37]

Acknowledgements

Funding for this research was provided by the Abdul Latif Jameel World Water and Food Systems Lab (J-WAFS) at MIT. This material is based upon work supported by the National Science Foundation Graduate Research Fellowship under Grant No. 1122374. We thank Matt Wolski of Daramic for providing us with polyporous separator samples. We thank Yuzhang Li and Nathan Corbin for productive and helpful discussions.

doi: 10.1016/j.joule.2019.02.003

Author Contributions

Conceptualization, N.L. and K.M.; Methodology, N.L.; Investigation, N.L.; Validation, Z.J.S.; Writing – Original Draft, N.L.; Writing – Review & Editing – N.L., K.W., and K.M.; Supervision. K.M.

Declaration of Interests

The authors declare no competing interests.

References

[1] Food and Agriculture Organization of United Nations. World fertilizer trends and outlook to 2020. Rome: 2017.

[2] Erisman JW, Sutton MA, Galloway J, Klimont Z, Winiwarter W. How a century of ammonia synthesis changed the world. Nat Geosci 2008;1:636–9. doi:10.1038/ngeo325.

[3] Giddey S, Badwal SPS, Munnings C, Dolan M. Ammonia as a Renewable Energy Transportation Media. ACS Sustain Chem Eng 2017;5:10231–9. doi:10.1021/acssuschemeng.7b02219.

[4] Nørskov J, Chen J. Sustainable Ammonia Synthesis: Exploring the scientific challenges associated with discovering alternative, sustainable processes for ammonia production. Dulles, VA: 2016.

[5] Kahrl F, Li Y, Su Y, Tennigkeit T, Wilkes A, Xu J. Greenhouse gas emissions from nitrogen fertilizer use in China. Environ Sci Policy 2010;13:688–94. doi:10.1016/j.envsci.2010.07.006.

[6] Institute for Industrial Productivity. Ammonia. Ind Effic Technol Database n.d. http://ietd.iipnetwork.org/content/ammonia (accessed August 14, 2018).

[7] Foster SL, Bakovic SIP, Duda RD, Maheshwari S, Milton RD, Minteer SD, et al. Catalysts for nitrogen reduction to ammonia. Nat Catal 2018;1:490–500. doi:10.1038/s41929-018-0092-7.

[8] Schiffer ZJ, Manthiram K. Electrification and Decarbonization of the Chemical Industry. Joule 2017;1:10–4. doi:10.1016/j.joule.2017.07.008.

[9] Chen JG, Crooks RM, Seefeldt LC, Bren KL, Bullock RM, Darensbourg MY, et al. Beyond fossil fuel–driven nitrogen transformations. Science 2018;360:eaar6611. doi:10.1126/science.aar6611.

[10] Bao D, Zhang Q, Meng F-L, Zhong H-X, Shi M-M, Zhang Y, et al. Electrochemical

doi: 10.1016/j.joule.2019.02.003

Reduction of N_2 under Ambient Conditions for Artificial N_2 Fixation and Renewable Energy Storage Using N_2/NH_3 Cycle. Adv Mater 2017;29:1604799. doi:10.1002/adma.201604799.

[11] Kong J, Lim A, Yoon C, Jang JH, Ham HC, Han J, et al. Electrochemical Synthesis of NH_3 at Low Temperature and Atmospheric Pressure Using a γ-Fe_2O_3 Catalyst. ACS Sustain Chem Eng 2017;5:10986–95. doi:10.1021/acssuschemeng.7b02890.

[12] Yang X, Nash J, Anibal J, Dunwell M, Kattel S, Stavitski E, et al. Mechanistic Insights into Electrochemical Nitrogen Reduction Reaction on Vanadium Nitride Nanoparticles. J Am Chem Soc 2018;140:13387–91. doi:10.1021/jacs.8b08379.

[13] Furuya N, Yoshiba H. Electroreduction of nitrogen to ammonia on gas-diffusion electrodes loaded with inorganic catalyst. J Electroanal Chem 1990;291:269–72.

[14] Lv C, Qian Y, Yan C, Ding Y, Liu Y, Chen G, et al. Defect Engineering Metal-Free Polymeric Carbon Nitride Electrocatalyst for Effective Nitrogen Fixation under Ambient Conditions. Angew Chemie Int Ed 2018;57:10246–50. doi:10.1002/anie.201806386.

[15] Tsuneto A, Kudo A, Sakata T. Lithium-mediated electrochemical reduction of high pressure N_2 to NH_3. J Electroanal Chem 1994;367:183–8. doi:10.1016/0022-0728(93)03025-K.

[16] McEnaney JM, Singh AR, Schwalbe JA, Kibsgaard J, Lin JC, Cargnello M, et al. Ammonia synthesis from N_2 and H_2O using a lithium cycling electrification strategy at atmospheric pressure. Energy Environ Sci 2017;10:1621–30. doi:10.1039/C7EE01126A.

[17] Ma J-L, Bao D, Shi M-M, Yan J-M, Zhang X-B. Reversible Nitrogen Fixation Based on a Rechargeable Lithium-Nitrogen Battery for Energy Storage. Chem 2017;2:525–32. doi:10.1016/j.chempr.2017.03.016.

[18] Kim K, Lee SJ, Kim D-Y, Yoo C-Y, Choi JW, Kim J-N, et al. Electrochemical Synthesis of Ammonia from Water and Nitrogen: A Lithium-Mediated Approach Using Lithium-Ion Conducting Glass Ceramics. ChemSusChem 2018;11:120–4. doi:10.1002/cssc.201701975.

[19] Cui X, Tang C, Zhang Q. A Review of Electrocatalytic Reduction of Dinitrogen to Ammonia under Ambient Conditions. Adv Energy Mater 2018;8:1800369. doi:10.1002/aenm.201800369.

[20] Kyriakou V, Garagounis I, Vasileiou E, Vourros A, Stoukides M. Progress in the Electrochemical Synthesis of Ammonia. Catal Today 2017;286:2–13. doi:10.1016/j.cattod.2016.06.014.

[21] Greenwood NN., Earnshaw A. Chemistry of the Elements. 2nd Editio. Elsevier; 1997.

[22] Greenlee LF, Renner JN, Foster SL. The Use of Controls for Consistent and Accurate Measurements of Electrocatalytic Ammonia Synthesis from Dinitrogen. ACS Catal 2018;8:7820–7. doi:10.1021/acscatal.8b02120.

[23] Zhang L, Ji X, Ren X, Luo Y, Shi X, Asiri AM, et al. Efficient Electrochemical N_2 Reduction to NH_3 on MoN Nanosheets Array under Ambient Conditions. ACS Sustain

doi: 10.1016/j.joule.2019.02.003

Chem Eng 2018:acssuschemeng.8b01438. doi:10.1021/acssuschemeng.8b01438.

[24] Zhang R, Zhang Y, Ren X, Cui G, Asiri AM, Zheng B, et al. High-Efficiency Electrosynthesis of Ammonia with High Selectivity under Ambient Conditions Enabled by VN Nanosheet Array. ACS Sustain Chem Eng 2018;6:9545–9. doi:10.1021/acssuschemeng.8b01261.

[25] Chen G-F, Cao X, Wu S, Zeng X, Ding L-X, Zhu M, et al. Ammonia Electrosynthesis with High Selectivity under Ambient Conditions via a Li^+ Incorporation Strategy. J Am Chem Soc 2017;139:9771–4. doi:10.1021/jacs.7b04393.

[26] Zhou F, Azofra LM, Ali M, Kar M, Simonov AN, McDonnell-Worth C, et al. Electro-synthesis of ammonia from nitrogen at ambient temperature and pressure in ionic liquids. Energy Environ Sci 2017;10:2516–20. doi:10.1039/C7EE02716H.

[27] Berger S, Braun S, Kalinowski H-O. NMR Spectroscopy of the Non-Metallic Elements. 2nd Editio. Bonn: John Wiley & Sons, Inc; 1988.

[28] Dabundo R, Lehmann MF, Treibergs L, Tobias CR, Altabet MA, Moisander PH, et al. The Contamination of Commercial $^{15}N_2$ Gas Stocks with ^{15}N–Labeled Nitrate and Ammonium and Consequences for Nitrogen Fixation Measurements. PLoS One 2014;9:e110335. doi:10.1371/journal.pone.0110335.

[29] Minteer SD, Christopher P, Linic S. Recent Developments in Nitrogen Reduction Catalysts: A Virtual Issue. ACS Energy Lett 2018:163–6. doi:10.1021/acsenergylett.8b02197.

[30] Wang H, Zhang W-D, Deng Z-Q, Chen M-C. Interaction of nitrogen with lithium in lithium ion batteries. Solid State Ionics 2009;180:212–5. doi:10.1016/j.ssi.2008.12.001.

[31] Peled E, Menkin S. Review—SEI: Past, Present and Future. J Electrochem Soc 2017;164:A1703–19. doi:10.1149/2.1441707jes.

[32] McFarlane EF, Tompkins FC. Nitridation of lithium. Trans Faraday Soc 1962;58:997. doi:10.1039/tf9625800997.

[33] Atkins P. Physical Chemistry. 6th Editio. New York: W.H. Freeman and Company; 1998.

[34] An SJ, Li J, Daniel C, Mohanty D, Nagpure S, Wood DL. The state of understanding of the lithium-ion-battery graphite solid electrolyte interphase (SEI) and its relationship to formation cycling. Carbon N Y 2016;105:52–76. doi:10.1016/j.carbon.2016.04.008.

[35] Bard AJ, Faulkner LR. Electrochemical Methods. Fundamentals and Applications. 2nd Editio. Phoenix: John Wiley & Sons, Inc; 2001.

[36] Verdouw H, Van Echteld CJA, Dekkers EMJ. Ammonia determination based on indophenol formation with sodium salicylate. Water Res 1978;12:399–402. doi:10.1016/0043-1354(78)90107-0.

[37] Yu X, Han P, Wei Z, Huang L, Gu Z, Peng S, et al. Boron-Doped Graphene for Electrocatalytic N_2 Reduction. Joule 2018;2:1–13. doi:10.1016/j.joule.2018.06.007.